Chemical Geology 457 (2017) 95–106

Contents lists available at ScienceDirect

Chemical Geology

journal homepage: www.elsevier.com/locate/chemgeo

Organically bound iodine as a bottom-water redox proxy: Preliminary validation and application

Xiaoli Zhou [a,b], Hugh C. Jenkyns [c], Wanyi Lu [a], Dalton S. Hardisty [d], Jeremy D. Owens [e], Timothy W. Lyons [f], Zunli Lu [a,*]

[a] Department of Earth Sciences, Syracuse University, Syracuse, NY, United States
[b] Department of Marine and Coastal Sciences, Rutgers University, New Brunswick, NJ, United States
[c] Department of Earth Sciences, University of Oxford, Oxford, UK
[d] Department of Geology and Geophysics, Woods Hole Oceanographic Institution, Woods Hole, MA, United States
[e] Department of Earth, Ocean and Atmospheric Science, Florida State University, Tallahassee, FL, United States
[f] Department of Earth Sciences, University of California, Riverside, CA, United States

ARTICLE INFO

Article history:
Received 2 December 2016
Received in revised form 19 February 2017
Accepted 15 March 2017
Available online 18 March 2017

Keywords:
I/TOC
Bottom water
OAE 2
Black shale
Baltic

ABSTRACT

Carbonate-associated iodine (I/Ca) has been used as a proxy of local, upper-ocean redox conditions, and has successfully demonstrated highly dynamic spatial and temporal patterns across different time scales of Earth history. To further explore the utility of iodine as a paleo-environmental proxy, we present here a new method of extracting organically bound iodine (I_{org}) from shale using volumes of samples on the order of tens of milligrams, thus offering the potential for high-resolution work across thin shale beds. The ratio of I_{org} to total organic carbon (I/TOC) in modern surface and subsurface sediments decreases with decreasing bottom-water oxygen, which may be used to reconstruct paleo-redox changes.

As a proof of concept, we evaluate the I/TOC proxy in Holocene sediments from the Baltic Sea, Landsort Deep (IODP 347) and discuss those data within a framework of additional independent redox proxies, e.g., iron speciation and [Mo]. The results imply that I/TOC may be sensitive to hypoxic–suboxic conditions, complementary to proxies sensitive to more reducing, anoxic–euxinic conditions. Then, we test the usage of I/TOC in sediments deposited during Late Cretaceous, Cenomanian–Turonian Oceanic Anoxic Event (OAE) 2 from ~94 million years ago (Ma). We generated I/TOC and I_{org} records from six OAE 2 sections: Tarfaya (Morocco), Furlo (central Italy), Demerara Rise (western equatorial Atlantic), Cape Verde Basin (eastern equatorial Atlantic), South Ferriby (UK), and Kerguelen Plateau (southern Indian Ocean), which provide a broad spatial coverage. Generally, I/TOC decreases over the interval recorded by the positive carbon-isotope excursion, the global signature of OAE 2, suggesting an expansion of more reducing bottom-water conditions and consistent with independent constraints from iron speciation and redox-sensitive trace-metals (e.g., Mo). Relatively higher I/TOC values (thus more oxic conditions) are recorded at two high latitude sites for OAE 2, supporting previous model simulations (cGENIE) that indicated higher bottom water oxygen concentrations in these regions. Our results also indicate that organic-rich and oxygenated seafloors are likely a major sink of iodine and correspondingly influence its global seawater inventory.

1. Introduction

1.1. Iodine marine geochemistry and iodine proxies

Iodine is a redox-sensitive element (e.g., Wong, 1980), and carbonate I/Ca is a relatively new proxy for redox reconstructions in the upper ocean, sensitive to the transition between oxic and suboxic ($[O_2] < 5$ μmol/kg; Gilly et al., 2013) conditions (Hardisty et al., 2014; Hardisty et al., 2017; Lu et al., 2010; Lu et al., 2016; Owens et al., 2017; Zhou et al., 2015). Sedimentary organic matter is a large iodine reservoir in Earth's crust (Muramatsu and Wedepohl, 1998). Previous work has demonstrated the potential for ratios of organic iodine to TOC to distinguish bottom water redox conditions by evaluating iodine contents of organic-rich sediments from anoxic and well-oxygenated basins (Calvert and Pedersen, 1993; Price and Calvert, 1973). In this study, we build on this context and explore the potential of using the ratio between organically bound iodine and total organic carbon (I/TOC) as a proxy for paleo-redox conditions in ancient organic-rich sediments.

* Corresponding author.
E-mail address: zunlilu@syr.edu (Z. Lu).

http://dx.doi.org/10.1016/j.chemgeo.2017.03.016
0009-2541/

Iodine concentrations in modern seawater are relatively uniform around 0.45 μmol/l (Elderfield and Truesdale, 1980). Iodate is thermodynamically stable and is the predominant iodine species in oxygenated seawater (Tsunogai, 1971; Wong, 1980). Iodate is slightly depleted in surface ocean waters, due to the uptake by phytoplankton, and remains at a constant concentration in a fully oxygenated water column (e.g., Bluhm et al., 2011). Marine planktons take up iodine in the surface ocean at an average stoichiometry of 140 ± 80 μmol/mol relative to carbon (I/TOC) (Elderfield and Truesdale, 1980), although the uptake mechanisms are not clear. The presence of iodide (the reduced iodine species) in the surface ocean may be associated with reduction of iodate mistaken for nitrate by the enzyme nitrate reductase (Tsunogai and Sase, 1969). However, Waite and Truesdale (2003) challenged this hypothesis, claiming that iodate reduction in some marine microalga could be independent of the presence or absence of nitrate reductase activity.

Iodine can be enriched in marine sediments relative to phytoplankton. The enrichment mainly happens at the seafloor rather than in the water column (Price and Calvert, 1973). Iodine concentrations in exported particles may even decrease while sinking through the water column (e.g., from 200–300 to 100–200 ppm; Brewer et al., 1980; Wong et al., 1976), a process that may be associated with oxidation of organic matter. At the seafloor, I/TOC values of surface sediments depend on the bottom water oxygen condition. Iodine is enriched in the organic fraction (not in mineral phases) of sediments deposited under well-oxygenated bottom water, yielding sediment I/TOC values up to ~2500 μmol/mol (Fig. 1) (Kennedy and Elderfield, 1987b; Price and Calvert, 1973). Locations with oxygen-depleted bottom waters have lower I/TOC (Price and Calvert, 1973), on the same order of magnitude as the average I/TOC in plankton (Elderfield and Truesdale, 1980). I/TOC decreases rapidly from surface to subsurface sediments (<1 m) at oxygenated sites, whereas the ratios remain relatively stable at sites with low bottom water oxygen contents (Price and Calvert, 1977). Price and Calvert (1973) predicted that the contrasting burial behavior of iodine in oxidizing versus reducing environments should be recorded in ancient sediments.

The measurements of sedimentary iodine concentrations in these earlier investigations (e.g., Price and Calvert, 1973) do not differentiate iodine associated with organic matter, carbonate or residual porewater, although organic matter was generally thought to drive the signals. To simplify discussion, we treat the total sedimentary iodine to organic carbon ratios presented in the literature as organic I (I/TOC). Thus, the data from our literature review compiled in Fig. 1 serve as an approximation rather than a quantitative calibration between oxygen and I/TOC. Echoing the conceptual steps taken during the development of the I/Ca proxy, we (1) optimized the method by developing a new scheme for extracting iodine associated with marine organic matter especially well-suited to paleo-environmental reconstruction, (2) validated the sensitivity of I/TOC to local anoxia in the Baltic Sea (Holocene) in the context of other well-established proxies, and (3) applied I/TOC to multiple geologic sections recording a prime example of large-scale global deoxygenation event in relatively deep geologic time (Cretaceous OAE 2).

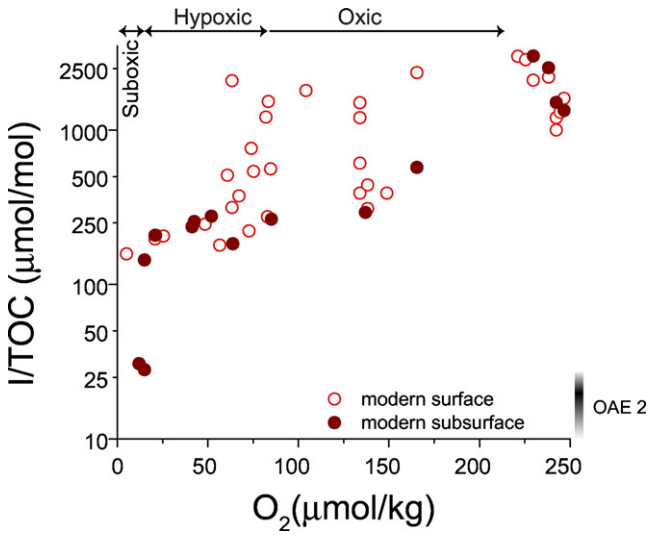

Fig. 1. I/TOC of modern marine sediments plotted with bottom-water oxygen concentration immediately overlying the seafloor. The open circles are surface sediments of the southwest African continental shelf (Price and Calvert, 1973) and tropical eastern Pacific and coastal areas of North Atlantic (Kennedy and Elderfield, 1987a). Closed circles are subsurface sediments from the Namibian shelf (Price and Calvert, 1977), Cascadia margin (Lu et al., 2008) and coastal areas of the tropical North Atlantic (Kennedy and Elderfield, 1987b). The range of OAE 2 I/TOC values are indicated as a gray shading. Note that the *y*-axis is log scale.

1.2. Holocene Baltic Sea

The Baltic Sea is among the world's largest anoxic basins. A sill at the Danish Straits acts as the only marine connection. This barrier, in combination with a positive water balance, leads to salinity stratification in the Baltic. Paleo-redox records indicate that transitions between water column hydrogen sulfide accumulation (euxinia) and less reducing redox state have occurred over the Holocene history of the Baltic Sea (Hardisty et al., 2016; Jilbert and Slomp, 2013). In this study, we evaluate I/TOC from Holocene sediments of the currently euxinic Baltic subbasin Landsort Deep—which is among the deepest and currently most reducing regions in the modern Baltic. These sediments were collected during IODP Expedition 347 (Andrén et al., 2015).

1.3. Cretaceous Oceanic Anoxic Event 2

Oceanic Anoxic Events (OAEs) are characterized by globally distributed marine deposition of organic-rich sediments known colloquially as black shales (Schlanger and Jenkyns, 1976; Jenkyns, 1980; Arthur et al., 1990; Jones and Jenkyns, 2001; Jenkyns, 2010). Black shales typically result from the combination of increased primary productivity coupled with enhanced preservation of organic matter in oxygen-depleted environments (e.g., Arthur et al., 1988; Demaison and Moore, 1980; Schlanger et al., 1987). The enhanced global burial of isotopically light organic carbon in terrestrial and marine reservoirs can be fingerprinted by a positive carbon-isotope excursion (CIE) spanning this event (Barclay et al., 2010; Hasegawa, 1997; Jarvis et al., 2011; Tsikos et al., 2004).

OAE 2 at the Cenomanian–Turonian boundary and other OAEs have been linked to the eruption of large igneous provinces (LIPs), which released CO_2 to the atmosphere, increasing atmospheric temperature and strengthening the hydrological cycle (e.g., Adams et al., 2010; Jenkyns, 2003; Kerr, 1998; Kuroda et al., 2007; Turgeon and Creaser, 2008). As a result, weathering rates of continental and exposed oceanic crust increased (Blättler et al., 2011; Jenkyns et al., 2017; Pogge von Strandmann et al., 2013), which delivered more nutrients to the oceans and stimulated marine productivity. Enhanced productivity shuttled more organic matter to greater depth, which in turn consumed more dissolved oxygen and induced oceanic deoxygenation in many regions—and the related enhanced preservation of the organic matter was a positive feedback that further favored the widespread burial of organic carbon (Jenkyns, 2003, 2010; Owens et al., 2016).

A wide range of proxies have been used to track water-column redox conditions. Biotic proxies such as foraminiferal assemblages provide indications of dissolved oxygen levels (Bomou et al., 2013; El-Sabbagh et al., 2011; Friedrich et al., 2006; Gertsch et al., 2010; Reolid et al., 2015; Takashima et al., 2009). Trace-metal enrichment and Fe-speciation data from bulk shale have also proven to be powerful tools to characterize redox changes during OAE 2 (van Helmond et al., 2014; Jenkyns et al., 2017; Junium et al., 2015; Owens et al., 2016; Poulton et al., 2015;

Scopelliti et al., 2006; Tribovillard et al., 2012; Westermann et al., 2014) and specifically allow us to track the presence or absence of euxinia during this event (Algeo and Lyons, 2006; Algeo and Tribovillard, 2009; Poulton and Canfield, 2005; Poulton and Canfeld, 2011). Biomarkers (e.g., isorenieratane) indicate euxinia in the photic zone in proto-North and South Atlantic Ocean during OAE 2 (Hetzel et al., 2011; Kuypers et al., 2002; Pancost et al., 2004; Sinninghe Damsté and Koster, 1998). Pyrite framboids of micron scale in some Tethyan sequences (Italy) similarly suggest at least intermittent presence of free hydrogen sulfide in the water column at the same time (Jenkyns et al., 2007).

2. Study sites

As a proof-of-concept, we measured I/TOC ratios in a Holocene core of organic-rich, laminated sediments from a currently euxinic sub-basin of the Baltic Sea, Landsort Deep—specifically, Site M0063 of Integrated Ocean Drilling Program (IODP) Expedition 347 (Andrén et al., 2015; Hardisty et al., 2016). The sediments from this study were piston cored. Further drilling details are available in Andrén et al. (2015). In some cases, samples were collected directly onboard within hours of coring and immediately heat-sealed in N_2-flushed bags. For most samples, however, the cores were immediately sealed on deck and stored at 4 °C until sample collection at MARUM in Bremen, Germany, where the subsamples were heat-sealed in N_2-flushed bags within hours of core exposure to ambient atmosphere. The sediments are organic-rich (ranging from 2 to 8 wt% TOC) and laminated throughout the interval of interest, consistent with infaunal asphyxiation excluding benthic habitation. During the IODP expedition, no calcified fossil assemblages were found throughout the entire sequence of interest (Andrén et al., 2015) and pore water modeling suggests that most of the observed carbonate represents authigenic Fe/Mn carbonate minerals (e.g., siderite and rhodochrosite; Hardisty et al., 2016).

Our samples span from a depth of 0.7 to 35 m and are all currently below the depth of active sulfate reduction and sulfide accumulation, with pore fluids hosting methane accumulation and extremely high alkalinity (up to 60 meq/l) from organic carbon remineralization (Andrén et al., 2015; Hardisty et al., 2016). We compared I/TOC data from Landsort Deep to previously published Mo concentrations and Fe speciation results from the same samples that indicate two past euxinic periods overlapping with intervals of enhanced organic-carbon burial (TOC up to 8 wt%) (Hardisty et al., 2016), providing both a multi-proxy comparison and a paleo-environmental context.

We studied OAE 2 in six sections that capture different environmental settings (Fig. 2). Five out of six sites are in the proto-North Atlantic or western Tethys, and one site is from the Southern Ocean. Although all of these sites contain layers of organic-rich sediments, local paleoenvironments vary, including different oceanographic settings, latitudes, water depths, and behaviors of redox-sensitive trace elements. This sample collection provides a comprehensive framework for exploring iodine cycling during OAE 2.

A well-preserved sequence of glauconitic calcareous sandstone and organic-rich chalks was cored at Ocean Drilling Program (ODP) Leg 183 Site 1138 on the western margin of the central Kerguelen Plateau, a large Early Cretaceous oceanic igneous plateau in the paleo-Indian Ocean sector of the Southern Ocean at a modern water depth of 1141 m (Coffin et al., 2000; Holbourn and Kuhnt, 2002; Murphy and Thomas, 2012). Hole 1138A was rotary cored in 1999 with ~698 m of sediments recovered, and six sedimentary lithologic units were defined (Coffin et al., 2000). Our samples fall in Unit IV, of Cenomanian to mid-Campanian age, right above the boundary of Unit IV and V (Coffin et al., 2000). The sediments from the Kerguelen Plateau studied here consist of ~1 m of black organic-rich claystones, virtually barren of calcareous foraminifera during OAE 2, although the overlying sediments contain moderately to well-preserved species (Holbourn and Kuhnt, 2002). The sediments we studied comprise mostly black shale, including the recovery stage of the CIE, as is shown in the organic-carbon isotope

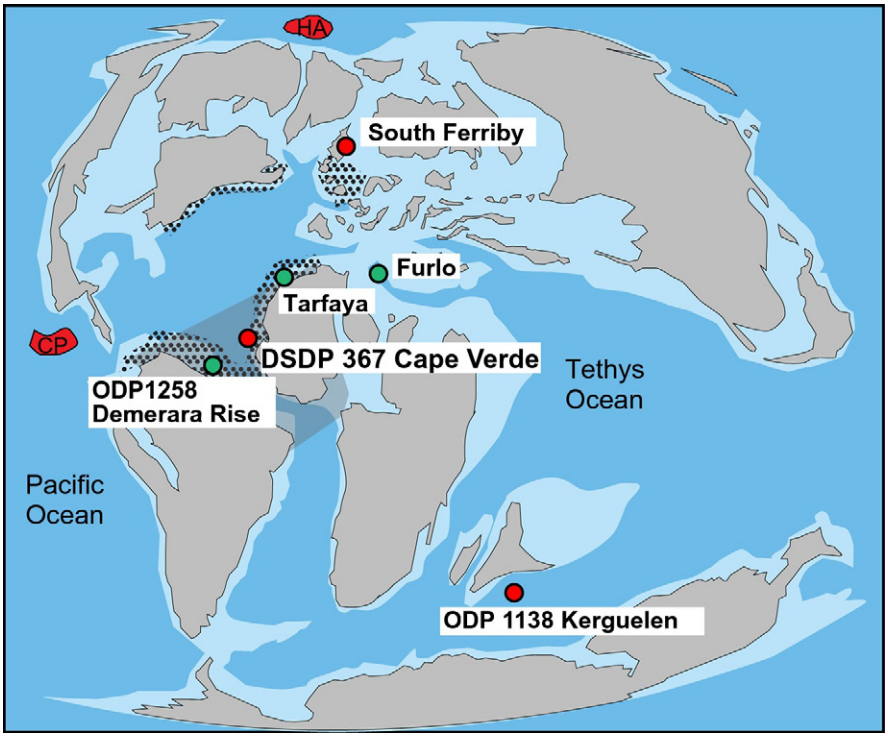

Fig. 2. Paleogeographic map for the Late Cretaceous. The beige shading represents continents, light blue neritic (shelf) seas, and dark blue deep seas. The six OAE 2 sections are divided into two groups; the green circles represent relatively reducing locations, and the red circles show relatively oxygenated ones. The full name is placed beside each site. The black dots mark the modeled upwelling regions from Topper et al. (2011), and the gray shading shows areas of prolonged euxinic conditions in the water column given in Jenkyns (2010). HA = High Arctic Large Igneous Province, CP = Caribbean Plateau.

data from Coffin et al. (2000) and Holbourn and Kuhnt (2002), as well as TOC and $CaCO_3$ percentage data. The average TOC content at this section is 7.7%, which is intermediate among all the six studied sites, which range from 2.4% to 24.0%. $CaCO_3$ percentage remains close to zero for most of the CIE and recovers to ~40% at the end of the excursion, suggesting low production and/or low preservation of carbonate during the event.

All other sites are in the pelagic proto-North and equatorial Atlantic Ocean and its continental margins. Deep Sea Drilling Project (DSDP) Leg 41 Site 367 is located at the base of the continental rise in the Cape Verde Basin, 330 km west of the African coast, at a current water depth of 4748 m and a paleodepth of 3700 m (Chenet and Francheteau, 1980; Lancelot et al., 1977; Westermann et al., 2014). The core was drilled in 1975, and seven lithological units were drilled. Our samples are from subunit 4a, which comprises mostly black shale, of late Aptian/eary Albian to early Turonian age (Lancelot et al., 1977). Detailed information can be found in Lancelot et al. (1977). The sediment in this study consists of black, organic-rich shale interbedded with silty turbidites and TOC that ranges from 4% to 48% (Jones et al., 2007; Lancelot et al., 1977). Clay and organic debris are common, with rare pyrite, traces of bioturbation, foraminifera and nannofossils (Lancelot et al., 1977). Our study of this core covers the early stage of the CIE and several meters below. The organic carbon isotopes and TOC data are from Kuypers et al. (2002). The maximum TOC value is the highest among the six studied sections.

Tarfaya, in southwest Morocco, is a section of organic-rich, shallow-marine sediments that span the Cenomanian–Turonian boundary (Kolonic et al., 2005). Core S57 (drilled by the Moroccan State Oil Company and Shell during exploration in the late 1970s and early 1980s; Kolonic et al., 2005) records the deepest part of the basin with a reconstructed paleo-water depth of ~250–300 m. The core comprises ~37 m of organic-rich calcareous sediment containing planktonic foraminifera and nannofossils, with light- and dark-colored layers that alternate at a decimeter scale (Tsikos et al., 2004). $\delta^{13}C$ and TOC data are from Tsikos et al. (2004). TOC (wt%) fluctuates between 0 and 15% for most of the section, with a peak value of 25% corresponding to the early stage of the CIE. Other dominant sedimentary components in this section include carbonate, finely dispersed biogenic silica, and clay (Leine, 1986; Tsikos et al., 2004).

The Furlo section of the pelagic Scaglia Bianca Formation was deposited at ~20°N in western Tethys, central Italy (Lanci et al., 2010). The lower 17.5 m of the section consists of rhythmically developed, light gray foraminiferal-nannofossil limestones, locally with pink, gray and black cherts—the latter associated with thin (sub-cm-scale) laminated black shale in parts of the section and TOC of up to ~20% (Gambacorta et al., 2015; Jenkyns et al., 2007; Mitchell et al., 2008; Mort et al., 2007a; Turgeon and Brumsack, 2006). This limestone sequence is overlain by the Bonarelli Level, recording the impact of OAE 2, characterized by interbedded black laminated organic-rich shale (TOC 0.5–18%), gray claystone, and brown radiolarian sand, with a total thickness of ~1 m. A low-resolution organic $\delta^{13}C$ record shows a gradual up-section rise from −26.5‰ to −25.5‰ in sediments below the Bonarelli Level, with values increasing abruptly to −23.5‰ at the onset of the positive CIE and fluctuating between −24 and −23‰ through that organic-rich interval (Jenkyns et al., 2007).

South Ferriby is located in Lincolnshire, northeast UK, and its sediments (chalk) were deposited on a shallow epicontinental pelagic shelf, adjacent to the proto-Atlantic Ocean. This section has been studied before, and carbon isotope and TOC data are from Jenkyns et al. (2007). The section comprises relatively condensed organic-lean foraminiferal-nannofossil carbonates with TOC mostly between 1 and 2%, interrupted by a thin (~10 cm) layer of organic-rich (max. TOC = ~8%) and laminated marls (Jenkyns et al., 2007; Pogge von Strandmann et al., 2013). The organic carbon-isotope profile gradually decreases upwards from −23 to −25‰ in the studied interval, capturing the recovering stage of the positive CIE.

Site 1258 (ODP Leg 207) is situated on the northwest slope of Demerara Rise adjacent to Suriname and French Guyana in the western equatorial Atlantic Ocean, currently located at a water depth of 3192 m (Erbacher et al., 2004; Friedrich et al., 2006). The Cenomanian to Turonian sequence consists mainly of laminated, organic-rich, black shales with local occurrence of limestones, chert, and phosphatic nodules and well-preserved fish debris (Hetzel et al., 2009). Clay content varies throughout the section, and the carbonate content is usually equal to or <50% in these organic-rich layers, with TOC contents of ~0.5 to 25% (Erbacher et al., 2004). The abundance of foraminifera varies drastically among the laminae (Nederbragt et al., 2007).

3. Methods

Various methods have been used previously to decompose and extract total iodine from sediment samples, such as dry ashing/alkaline fusion, microwave-assisted digestion, and combustion (Brown et al., 2005; Knapp et al., 1998; Romarís-Hortas et al., 2009; Tinggi et al., 2011). The sample masses required for these methods are usually larger than 100 mg (e.g., Hu et al., 2007; Knapp et al., 1998; Tullai et al., 1987), which are unsuitable for producing high-resolution paleo-records. Here, we develop a new method for extracting organic iodine using much smaller samples of ~20 mg. Extraction methods for modern environmental samples like soils (e.g. Hu et al., 2007) may not be ideal for ancient marine sediments for a number of reasons, such as the lack of a decarbonation step and possible residual iodine in refractory organic matter. We found, in a preliminary experiment, that older samples generally need longer digestion time for complete extraction of iodine. To address this issue, we chose two OAE 2 samples to identify the appropriate incubation time for the majority of the samples in this study. One is from a pre-OAE interval, the other is from within the OAE interval itself.

Fine powders of sediment were weighed on a microbalance, decarbonated by adding 3% (v/v) nitric acid and then thoroughly rinsed with DI (deionized) water for five times to remove any residual inorganic iodine. The decarbonated samples were transferred into Teflon vials and mixed with 2 ml of tetramethylammonium hydroxide (TMAH 25% in H_2O, Sigma-Aldrich TraceSELECT®). The vials were sealed tightly and heated in the oven at 90 °C. The heating and digestion of the two OAE test samples were carried out for 30 days to identify the appropriate heating time. The sealed vials were sonicated in a water bath for 1 h daily. Approximately 20 μl of solutions were subsampled from each Teflon vial and diluted with DI water for preservation in a refrigerator. Sub-sampling was carried out one to five times a week during the entire heating period. Iodine concentrations were measured in the sub-sampled solutions to determine the incubation time required for the OAE 2 samples. A potassium iodide solution was set up as a control and processed with the same method as the OAE 2 samples.

We also investigated the potential effect of sample mass on measured I/TOC values. Well-homogenized samples were weighed to ~5, 10, 20, 30, 40, and 50 mg and then treated following the same extraction method adopted for all the OAE 2 samples. Any systematic changes in I/TOC related to small sample weight would have implications on future higher resolution studies.

The bulk-rock samples from six OAE 2 sections were processed using the same method as described above, except that the sub-sampling was skipped, and the heating time was shortened to 20 days, which was demonstrated to be sufficient to completely extract iodine from the samples (Fig. 3). Before iodine analysis by ICP-MS, the stored solutions were mixed with a freshly made matrix containing internal standards. Potassium iodide (KI, Alfa Aesar, 99.99% in purity) was dissolved and diluted to make calibration standards. The standard deviation for each measurement was mostly <1% and was always <5%. I/TOC values were reported as measured I_{org} concentration over the TOC content. I_{org} values represent organically bound iodine content in the bulk rock.

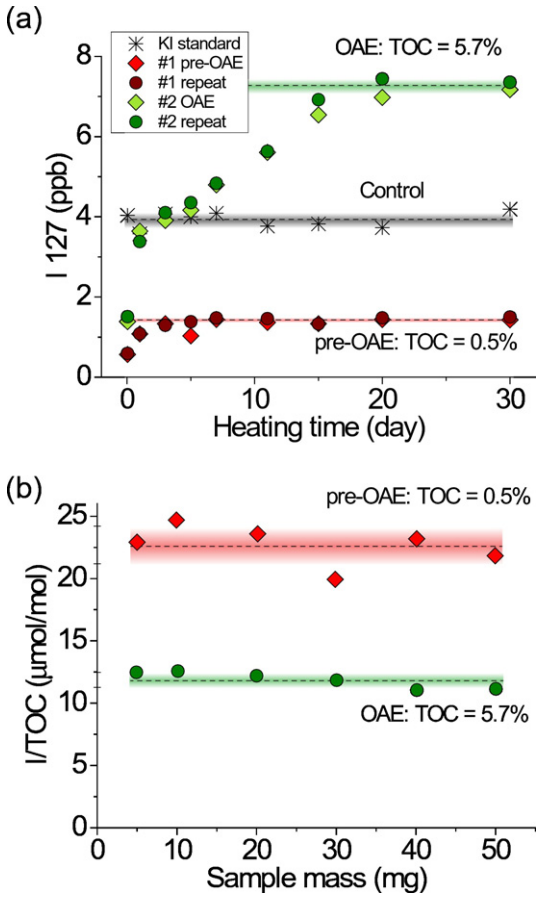

Fig. 3. (a). Iodine extraction results of the test run of two OAE 2 samples. Closed circles in maroon and diamonds in red represent the sample from the pre-OAE interval; closed circles in olive and diamonds in light green are the two identical samples from within the OAE interval; and the asterisks denote the KI standard. The plot shows changes in iodine concentration released from the samples with time. The dashed line and colored bars on top of each set of circles are the average value and standard deviation of the data, respectively. (b). Effect of sample mass on I/TOC values of the two OAE 2 samples. Diamonds in red and circles in green represent pre-OAE and OAE samples, respectively.

4. Results and discussion

4.1. Method development

The iodine concentrations in subsampled solutions increased in the first 20 days and remained almost constant afterwards (Fig. 3a). This result suggests that incubation for 20 days is sufficient to extract iodine from organic matter. The variation in KI concentrations (RSD = 5%) reflects the uncertainty in subsampling, preservation and measurement of iodine on the ICP-MS. The small variation suggests that there was no major loss through volatilization during the experiment (Fig. 3a).

The sample size experiment shows relatively constant I/TOC values with sample masses from 5 to 50 mg (Fig. 3b). The standard deviation of each set of I/TOC values are 6.6% and 5.1% for the pre-OAE and OAE samples respectively. All the OAE 2 samples were of ample size, and thus we chose a medium amount, ~20 mg, of well-homogenized powder for reconstructing stratigraphic trends. However, samples as small as 5 mg appear to be sufficient for future high-resolution work.

4.2. I/TOC as a qualitative bottom-water oxygenation proxy?

We begin this discussion by exploring the I/TOC proxy in light of previous work. The positive correlation between I/TOC and bottom-water oxygenation in recent sediments (Price and Calvert, 1973) (Fig. 1) reveals the potential for this proxy to reconstruct paleo-redox near the seafloor using ancient sediments. However, it is important to discuss the fundamentals and limitations of I/TOC as an oxygenation indicator in terms of (1) the mechanisms behind the correlation between surface-sediment I/TOC and bottom-water oxygen level, (2) preservation of primary I/TOC signal (and inferred oxygen gradients) during early diagenesis among different sites in shallow subsurface sediments, and (3) the influence of long-term burial.

The enrichment of iodine in oxic surface sediments (relative to marine plankton) has generally been linked to organic matter. Price and Calvert (1973) speculated that this enrichment is related to iodine sorption onto the organic fraction, controlled by unspecified enzyme reactions at the surface of dead cells that occur only in an oxidizing environment. Ullman and Aller (1985) proposed that IO_3^- may adsorb to Fe-oxyhydroxides on the surface of oxic sediments. A leaching experiment of surface sediments using a wide range of chemicals (organic/inorganic and acidic/base) led to the conclusion that iodine is specifically bound to N-iodoamides in polypeptides or chitin (Harvey, 1980). Francois (1987) reported laboratory experiments demonstrating that I/TOC of humic materials increased significantly after exposure to IO_3^- under oxygenated conditions. No increase of I/TOC was observed when I^- was added to humic materials, and oxyhydroxides only played a secondary role. Therefore, uptake of iodate by humic materials is probably the most likely mechanism for iodine enrichment in oxic surface sediment.

During early diagenesis, significant decreases in I/TOC are observed just below the sediment-water interface in sediments beneath an oxic water column, with values steadily decreasing to near-constant values within 0.5–2.5 m below the sediment-water interface, which was interpreted as preferential release of iodine relative to carbon (Price et al., 1970; Price and Calvert, 1977). Francois (1987) provided evidence for substitution of iodine by other anions (including HS^-) during early burial, causing the observed decrease in I/TOC. Low-oxygen sites show a more stable I/TOC depth profile in shallow subsurface sediments (Price and Calvert, 1977).

Higher I/TOC ratios seem to be preserved in subsurface sediments under relatively well-oxygenated bottom waters compared to oxygen-depleted waters, likely controlled by availability of humic materials and bottom-water iodate concentrations (Fig. 1). We do not recommend calibrating I/TOC values from modern surficial sediments to a specific bottom-water O_2 concentration to apply the calibration to deep time, since no known mechanism indicates chemical equilibrium between organically bound iodine and bottom water O_2 (Francois, 1987). However, it may be possible to evaluate relative changes in I/TOC at multiple ancient sites as a qualitative tracer for O_2 in the bottom water.

I/TOC data in ancient sediments cannot be compared directly with those in modern sediments due to iodine loss during diagenetic alteration of organic matter. I/TOC values of the OAE 2 samples are more than an order of magnitude lower than those in modern subsurface sediments of similar redox conditions (Fig. 1), possibly indicating preferential loss of iodine during the burial of organic matter over tens of millions of years (Francois, 1987). Nevertheless, there is potential for recording at least first-order spatial and temporal patterns in bottom-water oxygen using I/TOC values in the sediments deposited during OAEs and other ancient systems by analogy. OAE 2, characterized by widespread deposition of organic-rich sediments, along with modern–recent sediments from the Baltic, provides an ideal opportunity to test the fidelity of this new proxy. Given that the hypoxic–anoxic redox window is where this proxy behaves with greatest sensitivity, as documented in modern systems, I/TOC may be complementary to other proxies for bottom-water redox better suited to more strongly reducing conditions, such as Fe speciation and concentrations of redox-sensitive trace metals.

4.3. Proxy validation in Holocene sediments from the Baltic Sea

The Landsort Deep is a modern anoxic basin with bottom water hydrogen sulfide accumulation (euxinia) and is among the most reducing sub-basins in the modern Baltic Sea. Holocene sediments are laminated and have large variations in TOC, Fe geochemistry (Fe_T/Al, Fe_{HR}/Fe_T, and $(Fe_{py} + Fe_{AVS})/Fe_{HR}$: Fe_T = total iron; Fe_{HR} = highly reactive iron, specifically carbonate associated iron, ferric oxyhydroxides, magnetite, and pyrite; Fe_{py} = pyrite iron; Fe_{AVS} = acid volatile sulfides), and Mo concentrations confined to distinct intervals (Fig. 4). Elevated Fe_T/Al and Fe_{HR}/Fe_T ratios are diagnostic of anoxic water columns (Algeo and Lyons, 2006; Raiswell and Canfield, 1998), and when these Fe enrichments overlap with Mo enrichments of >25 and $(Fe_{py} + Fe_{AVS})/Fe_{HR}$ approaching 1, they are diagnostic of euxinic bottom waters (Algeo and Lyons, 2006; Poulton and Canfeld, 2011). Previous work has shown that the two periods of elevated TOC in our Landsort Deep profile overlap with large-scale Baltic anoxic events: the Medieval Climate Anomaly (MCA; 1.25–0.8 ka) and the Holocene Thermal Maximum (HTM; 8–4 ka) (Andrén et al., 2015; Hardisty et al., 2016). The elevated Fe and Mo data from these same periods (Fig. 4) uniquely indicate euxinia at Landsort Deep, analogous to water column conditions today (Hardisty et al., 2016; Noordmann et al., 2015).

Most of the I/TOC values through this section are <100 μmol/mol (Fig. 4), falling into the hypoxic to anoxic range based on the compiled literature data in Fig. 1. The Landsort Deep comparison of I/TOC, Fe speciation, and Mo paleo-redox proxies highlighted the critical fact that I/TOC values did not increase during periods independently inferred to be euxinic, which is consistent with iodate reduction preceding the reduction of Fe and sulfate (Rue et al., 1997). A cross-plot of I/TOC versus trace-metal proxies (Fig. 5) demonstrates that high I/TOC values are instead sensitive to the transition from hypoxic to anoxic condition while Fe speciation and Mo enrichment patterns distinguish between the presence of and lack of euxinia. This observation provides further validation for the ability of sedimentary I/TOC to record paleo-redox under less reducing conditions. I/TOC shows a pulsed increase at ~2–3 m during the interval between the two most recent euxinic periods overlapping with the MCA and modern sediments (Fig. 4). We emphasize that the pulse of high I/TOC is not within surficial sediments and is unlikely to be a diagenetic artifact of decreasing sedimentary iodine following progressive organic-matter remineralization (see previous section). The shallowest sample from this section is at 0.7 m with an I/TOC value of 102 μmol/mol, whereas the increase in I/TOC was observed directly below this sample (Fig. 4). Rather than diagenetic overprints, this I/TOC pattern likely reflects a period with relatively oxygenated bottom waters compared to the over- and underlying euxinic periods in the Landsort Deep.

4.4. Oceanographic patterns of I/TOC during pre- and post-OAE 2 intervals

We report I/TOC and I_{org} data across OAE 2 deposited at six sites (Figs. 2 and 6). $\delta^{13}C$ and TOC data are plotted for each site (Fig. 6). Firstly, we discuss the spatial pattern of I/TOC during the background—that is, above and below the OAE 2 sediment. Subsequently, we discuss the temporal changes of I/TOC at individual sites. A summary of multiple redox proxies for each site can be found in Table 1.

I/TOC values for the pre- and post-OAE intervals display a wide range, from ~1 to >50 μmol/mol, effectively separating the study sites into two groups. Sites with background I/TOC < 5 μmol/mol appear to be located at low latitudes (Tarfaya, Furlo and Demerara Rise), with the exception of the Cape Verde Basin. Based on these contrasting I/TOC values, we suggest that bottom water was more oxic at the high-latitude sites and Cape Verde Basin, before and after the OAE, whereas most low-latitude sites had relatively oxygen-depleted bottom waters.

Two sites at higher latitudes (Kerguelen Plateau and South Ferriby) display background I/TOC of ~15–50 μmol/mol. Benthic foraminiferal assemblages at Kerguelen Plateau suggest that the bottom waters might have been generally oxygenated with episodes of short-term dysoxia ($[O_2]$ = 4.5–45 μmol/kg; Rhoads and Morse, 1971) (Coffin et al., 2000; Holbourn and Kuhnt, 2002). The faunal data independently suggest a predominance of oxygenated conditions in agreement with relatively high I/TOC values at this site. No proxy data are available in the literature directly addressing the bottom-water conditions at South Ferriby, although several studies implied a latitudinal increase in seafloor oxygenation from the tropical sites to the North Atlantic and Northern Tethyan margins (van Helmond et al., 2014; Kuhnt and Wiedmann, 1995; Westermann et al., 2010, 2014). The high I/TOC at South Ferriby (northernmost marginal Atlantic site, in the European pelagic shelf sea) agrees with such a pattern. The background I/TOC at Cape Verde Basin is about 10–20 μmol/mol, which is lower than the range for Kerguelen Plateau and South Ferriby, indicating less oxic bottom waters before the OAE. Fe_{HR}/Fe_T values were steadily near 0.38 during that time (Westermann et al., 2014), a transitional state between the oxic and anoxic end-member sites, coinciding with its intermediate I/TOC values among the six sites.

Elevated concentrations of redox sensitive trace metals concentrations (e.g., Zn, V, and Mo) and repetitive deposition of laminated organic-rich sediments indicate suboxic to anoxic bottom waters in the Tarfaya Basin during and after OAE 2 (Kolonic et al., 2005), and the presence of isorenieratane and the high degree of pyritization in sediments indicate at least intermittent photic-zone euxinia at this site (Kolonic et al., 2005; Poulton et al., 2015). Detailed Fe-speciation data suggest that bottom-water anoxia/euxinia existed before OAE 2 at Tarfaya (Poulton et al., 2015), which agrees with the low I/TOC values determined in this study. In general, the low I/TOC background values at Tarfaya are consistent with suggestions of less oxygenated bottom waters at this site before and after the event. Transient occurrences of relatively oxic bottom waters, suggested by much higher resolution studies (Keller et al., 2008; Kolonic et al., 2005; Kuhnt et al., 2005), are not captured in our low-resolution I/TOC record.

I/TOC values are relatively low in sediments deposited before, during, and after OAE 2 at Demerara Rise and Furlo, consistent with anoxic

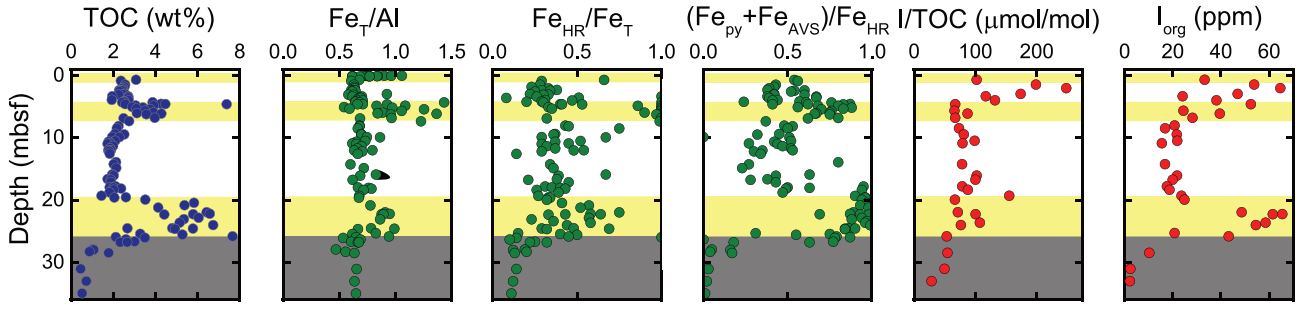

Fig. 4. TOC%, Fe_T/Al, Fe_{HR}/Fe_T, $(Fe_{py} + Fe_{AVS})/Fe_{HR}$, I/TOC, and I_{org} record for the upper 35 m of the Landsort Deep core in the Baltic Sea. Yellow boxes represent euxinic conditions, representing ~2 m, 4.3–7.3 m, and 19.5–26.75 m from the top to the bottom. The gray boxes indicate lacustrine sediments between 25 and 35 m. TOC% and Fe speciation data are from Hardisty et al. (2016). I/TOC and I_{org} data are from this study.

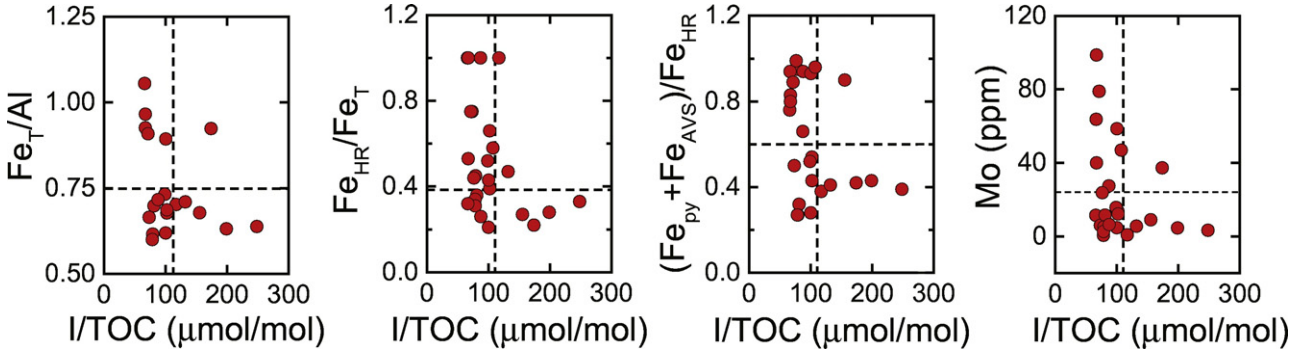

Fig. 5. Fe_T/Al, Fe_{HR}/Fe_T, $(Fe_{py} + Fe_{AVS})/Fe_{HR}$, and Mo concentration plotted against I/TOC through the upper 25 m of the Landsort Deep core in the Baltic Sea. The vertical dashed lines in each plot indicate I/TOC values at 115 μmol/mol, and horizontal lines in each plot represent Fe_T/Al, Fe_{HR}/Fe_T, $(Fe_{py} + Fe_{AVS})/Fe_{HR}$, and Mo concentration of 0.75, 0.38, 0.6, and 25, respectively (Hardisty et al., 2016). Fe_T/Al, Fe_{HR}/Fe_T, $(Fe_{py} + Fe_{AVS})/Fe_{HR}$, and Mo concentration above these thresholds suggest euxinic conditions.

to euxinic conditions as suggested by trace-metal data, $\delta^{15}N$, pyrite framboid size, biomarkers, and Fe-speciation results at these two sites (Hetzel et al., 2009; Jenkyns et al., 2007; Owens et al., 2016, 2017; Turgeon and Brumsack, 2006). The presence of the biomarkers isorenieratane and chlorobactane suggest photic-zone euxinia during OAE 2 at the relatively shallow Site 1260 on Demerara Rise, where ratios of lycopane to n-alkane much higher than those in modern OMZs indicate prolonged anoxia in the bottom water throughout the late Cenomanian to early Turonian (van Bentum et al., 2009). Similarly, at Furlo Fe speciation and Mo concentrations in black shales are consistent with intermittent, local ferruginous conditions prior to the event and euxinic conditions during the OAE itself (Bunte, 2009; Jenkyns et al., 2007; Owens et al., 2017; Westermann et al., 2014).

4.5. Temporal changes in local I/TOC during OAE 2

OAE 2 sediments, as defined by the $\delta^{13}C$ excursion, show lower I/TOC at all study sites (Fig. 6), most likely indicating less oxygenated bottom-water conditions due to widespread increase in planktonic carbon flux. The two high-latitude sites, Kerguelen and South Ferriby, have minimum I/TOC values of ~10–25 μmol/mol during the OAE interval, which are significantly higher than the minimum I/TOC values at the other sites (0–5 μmol/mol). Therefore, it seems likely that the relatively more oxygenated bottom waters found at higher latitudes persisted during the OAE itself.

The extent and timing of upper-ocean oxygenation changes indicated by I/Ca ratios are commonly not synchronous when calibrated against the carbon-isotope curve for OAE 2 (Zhou et al., 2015). Compared to I/Ca records for near-surface water conditions, I/TOC values for bottom-water signals show slightly better covariance with the $\delta^{13}C$ profile through the OAE interval at almost all sites. These data suggest that local bottom-water redox conditions were more synchronized with the patterns of global organic-carbon burial. This result is unsurprising, because upper-ocean oxygenation (recorded in I/Ca) is heavily influenced by interactions between the atmosphere and surface waters, whereas bottom-water oxygenation during the OAE should reflect widespread organic-matter burial and oxygen consumption in the oceanic interior.

4.6. I/TOC vs modeled seafloor oxygen

The latitudinal oceanographic pattern of background I/TOC agrees with the bottom-water oxygenation simulated in Earth System Model cGENIE for the Late Cretaceous with deeper Panama gateway (Fig. 7) (Monteiro et al., 2012). The three sites with high I/TOC values (Kerguelen Plateau, South Ferriby, and Cape Verde Basin) are located in or near areas with modeled bottom-water oxygen higher than 100 μmol/l (pre-OAE), whereas the other three sites are in areas with modeled seafloor oxygen below 50 μmol/l. Most parts of the proto-North Atlantic were probably anoxic around Cenomanian–Turonian time, because the deep water in the North Atlantic was likely formed at relatively low latitudes with warm surface water during the Cretaceous Period, hence containing less oxygen because of lower oxygen solubility in warm waters (Monteiro et al., 2012).

In the model of Monteiro et al. (2012), the northeast corner of the proto-Atlantic had relatively oxic water extending from the surface ocean to ~0.5 km (Zhou et al., 2015), consistent with the highest I/TOC at South Ferriby (Fig. 7). The Kerguelen Plateau was located at high southern latitudes, where lower temperatures could have favored higher levels of dissolved oxygen in seawater and possible formation of bottom water near this location. Nd-isotope results suggest deep-water formation in the Indian sector of the Southern Ocean at least from the late Albian to the late Cenomanian (Murphy and Thomas, 2012), which may have delivered O_2-rich deep water to Kerguelen—recorded as high I/TOC at this site.

The background I/TOC values (>10 μmol/mol) at Cape Verde are higher than expected, considering its low-latitude location. Interestingly, a modeled high O_2 anomaly on the seafloor appears persistently along the equatorial Western African margin, even in reconstructions where high-latitude bottom waters become almost anoxic (Monteiro et al., 2012). Regardless of the relatively high background I/TOC, given low pre-OAE Fe_{HR}/Fe_T and Mo/TOC ratios (Westermann et al., 2014) and the proximity to the modeled bottom-water O_2 anomaly, the Cape Verde region was probably susceptible to the influence of anoxic bottom water, as suggested by rapidly declining I/TOC during the OAE that, in the mid-stage of the event, reached levels similar to those at Demerara Rise.

4.7. Seawater iodine inventory

The marine iodine inventory could have changed during the OAE 2 global organic-carbon burial event, since the main output of iodine from seawater is organic matter in marine sediments (Muramatsu and Wedepohl, 1998). There is no consensus as to whether iodine would be drawn down as was the case with redox-sensitive trace metals (Algeo, 2004; Ma et al., 2014; Owens et al., 2016) or whether it would be more efficiently remobilized and recycled like phosphate (Mort et al., 2007b), regardless of differences in remobilization mechanisms of iodine and phosphate. The seawater iodine budget has implications for the interpretation of the carbonate I/Ca record, especially in deep time (Hardisty et al., 2017; Robbins et al., 2016), because I/Ca values are affected by the total iodine concentrations in seawater ($IO_3^- + I^-$). Organically bound iodine concentrations (I_{org}) may record, at least partially, the burial flux of iodine during OAE 2.

Average I_{org} values are highest at the Kerguelen and Cape Verde sites (Fig. 6). South Ferriby has relatively low I_{org} and low TOC, although it likely was relatively well oxygenated. These observations may indicate that the ideal sedimentary iodine sink in the global ocean is relatively

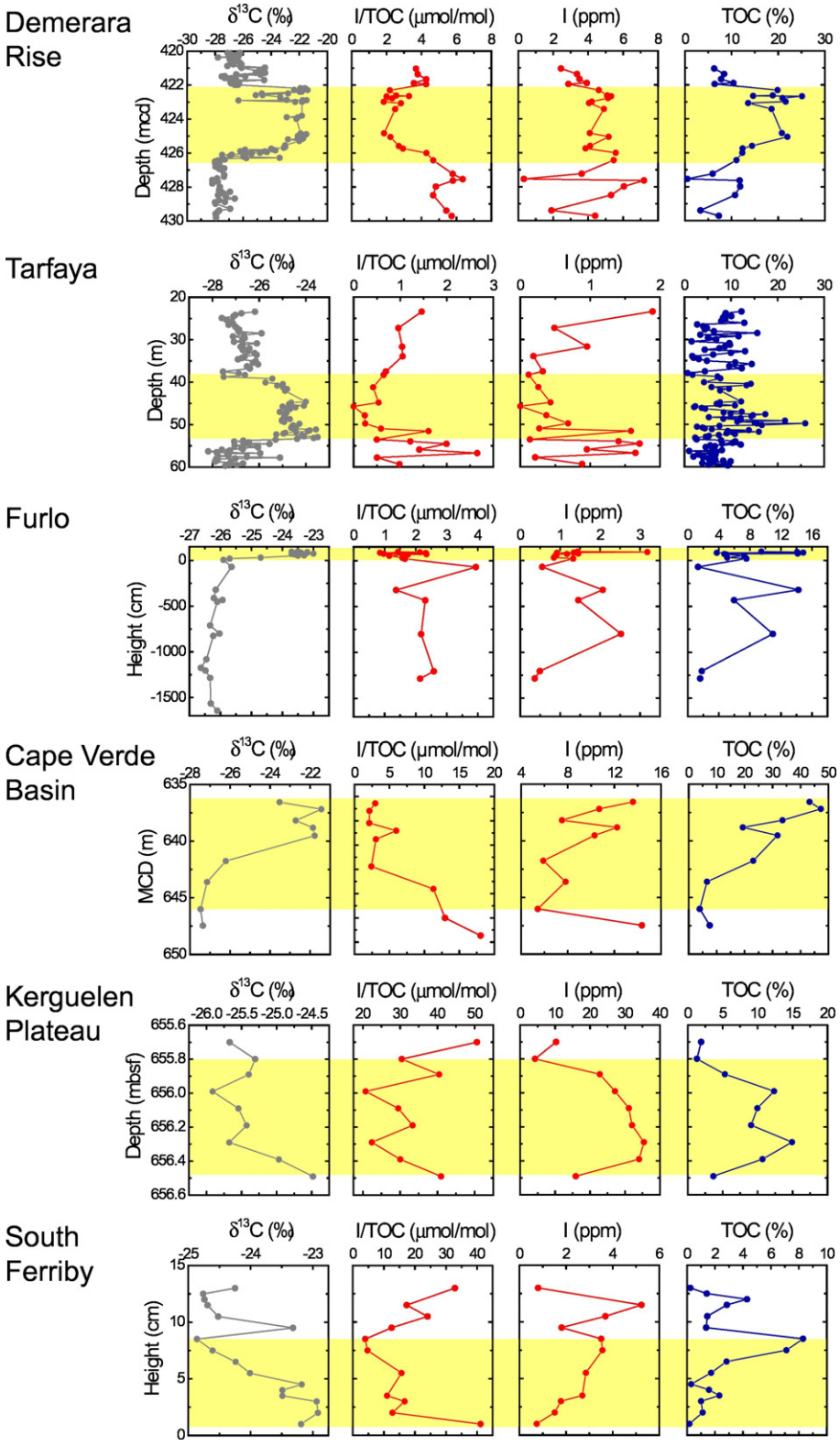

Fig. 6. Stratigraphic records of $\delta^{13}C$, I/TOC, I_{org}, and TOC at the six study sites. I/TOC and I_{org} data are from this study, $\delta^{13}C$ and TOC data are from Coffin et al. (2000) and Holbourn and Kuhnt (2002) for ODP Site Kerguelen Plateau; Kuypers et al. (2002) for DSDP Site 367 in the Cape Verde Basin; Tsikos et al. (2004) for site Tarfaya; Erbacher et al. (2005) for ODP Site 1258 on Demerara Rise; and Jenkyns et al. (2007) for sites Furlo and South Ferriby. The yellow boxes bracket the CIE or part of the CIE at each site.

oxic and organic-rich settings, because strong iodine enrichments in surface sediments may require both high bottom-water iodate concentrations and abundant humic materials (Francois, 1987). If this is true, the global marine iodine budget may be stabilized by the negative feedback between increasing organic-matter production and decreasing areas of oxic seafloor. I_{org} was relatively elevated at Kerguelen and Cape Verde during the OAE, regardless of decreasing I/TOC, possibly due to stronger iodine enrichment driven by more abundant organic matter

Table 1
Summary of redox proxy observations for OAE 2 at study sites.

Site	Proxies	Pre-CIE	CIE	Post-CIE	References
Demerara Rise	I/Ca	Low I/Ca values			Zhou et al., 2015
	Iron speciation	Fe_{HR}/Fe_T higher than 0.38	Fe_{HR}/Fe_T higher than 0.38	Fe_{HR}/Fe_T higher than 0.38	Hetzel et al., 2006; Böttcher et al., 2006
	Trace metals	Low Mn content	Enrichment of Fe and Co, low Mn content	Low Mn content	Hetzel et al., 2009
	Biomarkers	Presence of lycopane	Presence of Isorenieratane, chlorobactane and lycopane	Presence of lycopane	van Bentum et al., 2009
	Foraminiferal assemblages		Low abundance in benthic foraminifera		Friedrich et al., 2006
Tarfaya	I/Ca	Low I/Ca values	Low I/Ca values	Low I/Ca values	Zhou et al., 2015
	Iron speciation		Fe_{HR}/Fe_T higher than 0.38, Fe_{Py}/Fe_{HR} fluctuating around 0.7 (0.4–0.9)		Poulton et al., 2015
	Biomarkers		Presence of Isorenieratane and chlorobactane	Presence of Isorenieratane and chlorobactane	Kolonic et al., 2005; Poulton et al., 2015
	Foraminiferal assemblages	Low abundance of benthic foraminifera			Kuhnt et al., 2005
Furlo	I/Ca	Low I/Ca values		Low I/Ca values	Owens et al., 2017
	Iron speciation	Fe_{HR}/Fe_T higher than 0.38, Fe_{Py}/Fe_{HR} lower than 0.8	Fe_{HR}/Fe_T higher than 0.38, Fe_{Py}/Fe_{HR} lower than 0.8		Westermann et al., 2014
	Trace metals		High U, V, Mo contents, low Mn content		Turgeon and Brumsack, 2006
Cape Verde Basin	Iron speciation		Fe_{HR}/Fe_T higher than 0.38, Fe_{Py}/Fe_{HR} between 0.1 and 0.7		Westermann et al., 2014
	Trace metals	High V contents	High U, V, Mo contents		Westermann et al., 2014
Kerguelen Plateau	Foraminiferal assemblages		Barren foraminifera		Holbourn and Kuhnt, 2002
South Ferriby	I/Ca	High I/Ca suggest relatively oxygenated upper ocean	I/Ca peaks may suggest local water oxygenation or invasion of iodate-rich waters	High I/Ca suggest relatively oxygenated upper ocean	Zhou et al., 2015
	Trace metals	High Mn content	Low Mn content suggest dysoxic bottom water	High Mn content	Turgeon and Brumsack, 2006

on the seafloor, which overcame the effect of deoxygenation (lower bottom water iodate level). I_{org} shows better correlation with TOC at Kerguelen and South Ferriby than at other sites during OAE 2, which may suggest that TOC becomes the main control for iodine enrichment when the bottom water is oxygenated (Fig. 8). At Furlo, Demerara Rise, and Tarfaya, I_{org} values either remain at the same level as those of the pre-OAE interval or decrease during the OAE. Thus, regions with more reducing bottom waters (i.e. low iodate level) were not able to enhance iodine burial even with high local fluxes of organic matter, further supporting the idea that both bottom-water iodate and organic matter are prerequisites for an efficient sedimentary iodine sink. I_{org} and I/TOC are discussed separately as indicators for iodine inventory and oceanic oxygenation, respectively, but these parameters are likely influenced by both iodine budget and bottom-water O_2—and likely additional factors. Quantitative reconstructions teasing apart these intertwined parameters during the OAE will require future work.

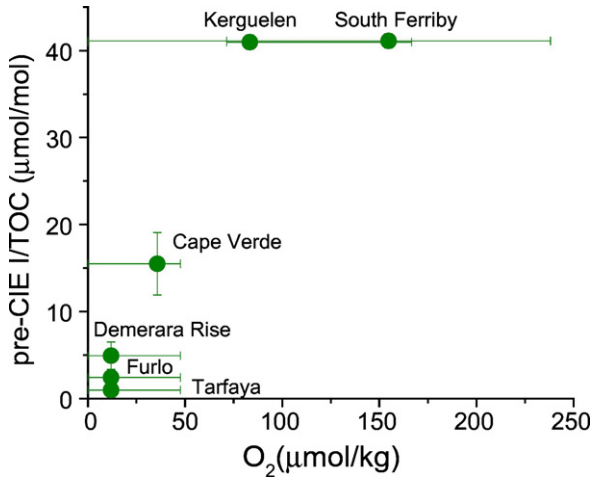

Fig. 7. Pre-CIE average I/TOC values plotted against modeled bottom-water oxygen for the Late Cretaceous with a deeper Panama, after Monteiro et al. (2012). Vertical error bars represent the standard deviation of the average pre-CIE I/TOC value from each site; horizontal error bars represent values calculated from the surrounding modeled bottom-water O_2 concentrations of each site.

5. Conclusions

Ratios of organically bound iodine (I_{org}) to total organic carbon (I/TOC) correlate empirically with bottom-water oxygenation in the

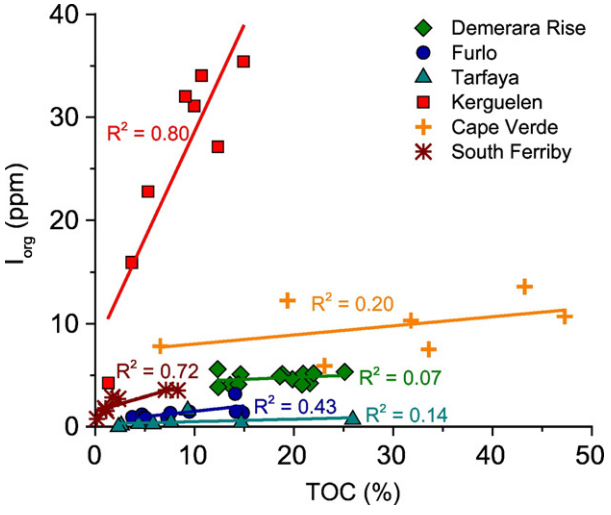

Fig. 8. Organically bound iodine concentration in bulk sediment (I_{org}) plotted against corresponding TOC content for samples deposited during OAE 2. I_{org} data are from this study; TOC data are from published papers. Diamonds in green, circles in royal blue, triangles in dark cyan, squares in red, plus signs in orange, and asterisks in maroon colors represent the sites of Demerara Rise, Furlo, Tarfaya, Kerguelen Plateau, Cape Verde Basin, and South Ferriby, respectively. The colored lines across each data set are linear fittings with R^2 indicated in an adjacent position.

modern ocean, despite uncertainties about the specific mechanistic controls. We developed a method to extract organic iodine from small volumes of sediments to explore the potential of I/TOC as a paleo-redox proxy, and the small samples permit high-resolution reconstructions. We began by testing this proxy in Holocene sediments of the Baltic Sea. The results indicate that I/TOC is sensitive to hypoxic–anoxic conditions, thus providing an important complement to well-established metal proxies best suited to anoxic–euxinic conditions. I/TOC data from six sites recording the Cenomanian–Turonian OAE 2 showed relatively more oxic conditions at high-latitude sites, consistent with other redox indicators and model simulations. Bottom waters became more reducing during OAE 2 at all sites, and this relationship is expressed in lower I/TOC values. Compared to upper-ocean oxygenation recorded in carbonate I/Ca ratios, temporal changes in bottom-water conditions were relatively synchronous with increased global organic-carbon burial and oxygen utilization in the ocean interior during OAE 2. Total organically bound iodine content did not show consistent changes through the OAE 2 interval among different sites, so no firm conclusions as to the possible extent of global iodine burial can be drawn from the available data. However, our data suggest that relatively organic-rich sediments deposited under oxygenated bottom-water conditions may be an important sink for seawater iodine on a global scale.

Acknowledgements

XZ, WL and ZL are supported by NSF EAR-1349252 and OCE-1232620. DH and TWL acknowledge support from the Geobiology and Low-temperature Geochemistry (GG) Program of NSF. DH would like to acknowledge a Schlanger Ocean Drilling Fellowship.

References

Adams, D.D., Hurtgen, M.T., Sageman, B.B., 2010. Volcanic triggering of a biogeochemical cascade during Oceanic Anoxic Event 2. Nat. Geosci. 3:201–204. http://dx.doi.org/10.1038/Ngeo743.

Algeo, T.J., 2004. Can marine anoxic events draw down the trace element inventory of seawater? Geology 32:1057–1060. http://dx.doi.org/10.1130/G20896.1.

Algeo, T.J., Lyons, T.W., 2006. Mo–total organic carbon covariation in modern anoxic marine environments: implications for analysis of paleoredox and paleohydrographic conditions. Paleoceanography 21, PA1016. http://dx.doi.org/10.1029/2004PA001112.

Algeo, T.J., Tribovillard, N., 2009. Environmental analysis of paleoceanographic systems based on molybdenum-uranium covariation. Chem. Geol. 268:211–225. http://dx.doi.org/10.1016/j.chemgeo.2009.09.001.

Andrén, T., Jørgensen, B.B., Cotterill, C., Green, S., Andrén, E., Ash, J., Bauersachs, T., Cragg, B., Fanget, A.-S., Fehr, A., Granoszewski, W., Groeneveld, J., Hardisty, D., Herrero-Bervera, E., Hyttinen, O., Jensen, J.B., Johnson, S., Kenzler, M., Kotilainen, A., Kotthoff, U., Marshall, I.P.G., Martin, E., Obrochta, S., Passchier, S., Quintana Krupinski, N., Riedinger, N., Slomp, C., Snowball, I., Stepanova, A., Strano, S., Torti, A., Warnock, J., Xiao, N., Zhang, R., 2015. Site M0063. In: Andrén, T., Jørgensen, B.B., Cotterill, C., Green, S., the Expedition 347 Scientists (Eds.), Proc. IODP, 347: College Station, TX (Integrated Ocean Drilling Program) http://dx.doi.org/10.2204/iodp.proc.347.107.2015.

Arthur, M.A., Dean, W.E., Pratt, L.M., 1988. Geochemical and climatic effects of increased marine organic carbon burial at the Cenomanian/Turonian boundary. Nature 335:714–717. http://dx.doi.org/10.1038/335714a0.

Arthur, M.A., Jenkyns, H.C., Brumsack, H.J., Schlanger, S.O., 1990. Stratigraphy, geochemistry, and paleoceanography of organic carbon-rich Cretaceous sequences. In: Ginsburg, R.N., Beaudoin, B. (Eds.), Cretaceous Resources, Events and Rhythms. Kluwer Academic Publishers, The Netherlands, pp. 75–119.

Barclay, R.S., McElwain, J.C., Sageman, B.B., 2010. Carbon sequestration activated by a volcanic CO_2 pulse during Ocean Anoxic Event 2. Nat. Geosci. 3:205–208. http://dx.doi.org/10.1038/ngeo757.

van Bentum, E.C., Hetzel, A., Brumsack, H.J., Forster, A., Reichart, G.J., Damste, J.S.S., 2009. Reconstruction of water column anoxia in the equatorial Atlantic during the Cenomanian-Turonian oceanic anoxic event using biomarker and trace metal proxies. Palaeogeogr. Palaeoclimatol. Palaeoecol. 280:489–498. http://dx.doi.org/10.1016/j.palaeo.2009.07.003.

Blättler, C.L., Jenkyns, H.C., Reynard, L.M., Henderson, G.M., 2011. Significant increases in global weathering during Oceanic Anoxic Events 1a and 2 indicated by calcium isotopes. Earth Planet. Sci. Lett. 309:77–88. http://dx.doi.org/10.1016/j.epsl.2011.06.029.

Bluhm, K., Croot, P.L., Huhn, O., Rohardt, G., Lochte, K., 2011. Distribution of iodide and iodate in the Atlantic sector of the southern ocean during austral summer. Deep-Sea Research Part II-Topical Studies in Oceanography 58:2733–2748. http://dx.doi.org/10.1016/j.dsr2.2011.02.002.

Bomou, B., Adatte, T., Tantawy, A.A., Mort, H., Fleitmann, D., Huang, Y., Föllmi, K.B., 2013. The expression of the Cenomanian-Turonian oceanic anoxic event in Tibet. Palaeogeogr. Palaeoclimatol. Palaeoecol. 369:466–481. http://dx.doi.org/10.1016/j.palaeo.2012.11.011.

Böttcher, M.E., Hetzel, A., Brumsack, H., Schipper, A., 2006. Sulfur-iron-carbon geochemistry in sediments of the Demerara Rise. In: Mosher, D.C., Erbacher, J., Malone, M.J. (Eds.), Proceedings of the Ocean Drilling Program, Scientific Results. 207. http://dx.doi.org/10.2973/odp.proc.sr.207.108.2006.

Brewer, P.G., Nozaki, Y., Spencer, D.W., Fleer, A.P., 1980. Sediment trap experiments in the deep North Atlantic - isotopic and elemental fluxes. J. Mar. Res. 38, 703–728.

Brown, C.F., Geiszler, K.N., Vickerman, T.S., 2005. Extraction and quantitative analysis of iodine in solid and solution matrixes. Anal. Chem. 7, 7062–7066.

Bunte, von F.A., 2009. Geochemical Signatures of Black Shales Deposited during Oceanic Anoxic Event 2 (Cenomanian/Turonian) in the Tropical Atlantic (Demerara Rise, ODP Leg 207) and in Northern Germany (Wunstorf). Dissertation. Carl von Ossietzky Universität Oldenburg.

Calvert, S.E., Pedersen, T.F., 1993. Geochemistry of recent oxic and anoxic marine sediments: implications for the geological record. Mar. Geol. 113:67–88. http://dx.doi.org/10.1016/0025-3227(93)90150-T.

Chenet, P.Y., Francheteau, J., 1980. Bathymetric reconstruction method: application to the Central Atlantic Basin between 10°N and 40°N. Initial Rep. Deep Sea Drill. Proj. 51–53:231–243. http://dx.doi.org/10.2973/dsdp.proc.515253.171.1980.

Coffin, M.F., Frey, F.A., Wallace, P.J., 2000. 6. Site 1138: Proceedings of the Ocean Drilling Program, Initial Reports. 183. http://dx.doi.org/10.2973/odp.proc.ir.183.106.2000.

Demaison, G.J., Moore, G.T., 1980. Anoxic environments and oil source bed genesis. Org. Geochem. 2:9–31. http://dx.doi.org/10.1016/0146-6380(80)90017-0.

Elderfield, H., Truesdale, W., 1980. On the biophilic nature of iodine in seawater. Earth Planet. Sci. Lett. 50:105–114. http://dx.doi.org/10.1016/0012-821X(80)90122-3.

El-Sabbagh, A., Tantawy, A.A., Keller, G., Khozyem, H., Spangenberg, J., Adatte, T., Gertsch, B., 2011. Stratigraphy of the Cenomanian–Turonian Oceanic Anoxic Event OAE 2 in shallow shelf sequences of NE Egypt. Cretac. Res. 32:705–722. http://dx.doi.org/10.1016/j.cretres.2011.04.006.

Erbacher, J., Mosher, D.C., Malone, M.J., 2004. 5. Site 1258: Proceedings of the Ocean Drilling Program Initial Reports. 207. http://dx.doi.org/10.2973/odp.proc.ir.207.105.2004.

Erbacher, J., Friedrich, O., Wilson, P.A., Birch, H., Mutterlose, J., 2005. Stable organic carbon isotope stratigraphy across Oceanic Anoxic Event 2 of Demerara Rise, western tropical Atlantic. Geochem. Geophys. Geosyst. 6, Q06010. http://dx.doi.org/10.1029/2004gc000850.

Francois, R., 1987. The influence of humic substances on the geochemistry of iodine in nearshore and hemipelagic marine-sediments. Geochim. Cosmochim. Acta 51:2417–2427. http://dx.doi.org/10.1016/0016-7037(87)90294-8.

Friedrich, O., Erbacher, J., Mutterlose, J., 2006. Paleoenvironmental changes across the Cenomanian/Turonian Boundary Event (Oceanic Anoxic Event 2) as indicated by benthic foraminifera from the Demerara Rise (ODP Leg 207). Re Micropaleontol. 49:121–139. http://dx.doi.org/10.1016/j.revmic.2006.04.003.

Gambacorta, G., Jenkyns, H.C., Russo, F., Tsikos, H., Wilson, P.A., Faucher, G., Erba, E., 2015. Carbon- and oxygen-isotope records of mid-Cretaceous Tethyan pelagic sequences from the Umbria–Marche and Belluno Basins (Italy). Newsl. Stratigr. 48:299–323. http://dx.doi.org/10.1127/nos/2015/0066.

Gertsch, B., Keller, G., Adatte, T., Berner, Z., Kassab, A., Tantawy, A., El-Sabbagh, A., Stueben, D., 2010. Cenomanian–Turonian transition in a shallow water sequence of the Sinai, Egypt. Int. J. Earth Sci. 99:165–182. http://dx.doi.org/10.1007/s00531-008-0374-4.

Gilly, W.F., Beman, M., Litvin, S.Y., Robison, B.H., 2013. Oceanographic and biological effects of shoaling of the Oxygen Minimum Zone. Annu. Re Mar. Sci. 5:393–420. http://dx.doi.org/10.1146/annurev-marine-120710-100849.

Hardisty, D.S., Lu, Z., Planavsky, N.J., Bekker, A., Philippot, P., Zhou, X., Lyons, T.W., 2014. An iodine record of Paleoproterozoic surface ocean oxygenation. Geology 42:619–622. http://dx.doi.org/10.1130/G35439.1.

Hardisty, D.S., Riedinger, N., Planavsky, N.J., Asael, D., Andrén, T., Jørgensen, B.B., Lyons, T.W., 2016. A Holocene history of dynamic water column redox conditions in the Landsort Deep, Baltic Sea (IODP Expedition 347). Am. J. Sci. 216:713–745. http://dx.doi.org/10.2475/08.2016.01.

Hardisty, D.S., Lu, Z., Bekker, A., Diamond, C.W., Gill, B.C., Jiang, G., Kah, L.C., Knoll, A.H., Loyd, S.J., Osburn, M.R., Planavsky, N.J., Wang, C., Zhou, X., Lyons, T.W., 2017. Perspectives on Proterozoic surface ocean redox from iodine contents in ancient and recent carbonate. Earth Planet. Sci. Lett. 463:159–170. http://dx.doi.org/10.1016/j.epsl.2017.01.032.

Harvey, G.R., 1980. A study of the chemistry of iodine and bromine in marine sediments. Mar. Chem. 8:327–332. http://dx.doi.org/10.1016/0304-4203(80)90021-3.

Hasegawa, T., 1997. Cenomanian-Turonian carbon isotope events recorded in terrestrial organic matter from northern Japan. Palaeogeogr. Palaeoclimatol. Palaeoecol. 130:251–273. http://dx.doi.org/10.1016/S0031-0182(96)00129-0.

van Helmond, N.A.G.M., Ruvalcaba Baroni, I., Sluijs, A., Sinninghe Damsté, J.S., Slomp, C.P., 2014. Spatial extent and degree of oxygen depletion in the deep proto-North Atlantic basin during Oceanic Anoxic Event 2. Geochem. Geophys. Geosyst. 15:4254–4266. http://dx.doi.org/10.1002/2014GC005528.

Hetzel, A., Brumsack, H.-J., Schnetger, B., Böttcher, M.E., 2006. Inorganic geochemical characterization of lithologic units recovered during ODP Leg 207 (Demerara Rise). In: Mosher, D.C., Erbacher, J., Malone, M.J. (Eds.), Proc. ODP, Sci. Results, 207: College Station, TX (Ocean Drilling Program):pp. 1–37 http://dx.doi.org/10.2973/ odp.proc.sr.207.107.2006.

Hetzel, A., Bottcher, M.E., Wortmann, U.G., Brumsack, H.J., 2009. Paleo-redox conditions during OAE 2 reflected in Demerara Rise sediment geochemistry (ODP Leg 207). Palaeogeogr. Palaeoclimatol. Palaeoecol. 273:302–328. http://dx.doi.org/10.1016/j.palaeo.2008.11.005.

Hetzel, A., März, C., Vogt, C., Brumsack, H.J., 2011. Geochemical environment of Cenomanian - Turonian black shale deposition at Wunstorf (northern Germany). Cretac. Res. 32:480–494. http://dx.doi.org/10.1016/j.cretres.2011.03.004.

Holbourn, A., Kuhnt, W., 2002. Cenomanian–Turonian palaeoceanographic change on the Kerguelen Plateau: a comparison with Northern Hemisphere records. Cretac. Res. 23: 333–349. http://dx.doi.org/10.1006/cres.2002.1008.
Hu, Q.H., Moran, J.E., Blackwood, V., 2007. Geochemical cycling of iodine species in soils. In: Preedy, V.R.B., Gerard, N., Watson, R.R. (Eds.), Comprehensive Handbook of Iodine: Nutritional, Biochemical, Pathological and Therapeutic Aspects. Elsevier Inc, Oxford, UK, pp. 93–105.
Jarvis, I., Lignum, J.S., Gröcke, D.R., Jenkyns, H.C., Pearce, M.A., 2011. Black shale deposition, atmospheric CO_2 drawdown and cooling during the Cenomanian-Turonian Oceanic Anoxic Event (OAE 2). Paleoceanography 26, PA3201. http://dx.doi.org/10.1029/2010PA002081.
Jenkyns, H.C., 1980. Cretaceous anoxic events: from continents to oceans. J. Geol. Soc. 137: 171–188. http://dx.doi.org/10.1144/gsjgs.137.2.0171.
Jenkyns, H.C., 2003. Evidence for rapid climate change in the Mesozoic-Palaeogene greenhouse world. Philosophical Transactions of the Royal Society A-Mathematical Physical and Engineering Sciences 361:1885–1916. http://dx.doi.org/10.1098/rsta.2003.1240.
Jenkyns, H.C., 2010. Geochemistry of oceanic anoxic events. Geochem. Geophys. Geosyst. 11, Q03004. http://dx.doi.org/10.1029/2009gc002788.
Jenkyns, H.C., Matthews, A., Tsikos, H., Erel, Y., 2007. Nitrate reduction, sulfate reduction, and sedimentary iron isotope evolution during the Cenomanian-Turonian oceanic anoxic event. Paleoceanography 22, PA3208. http://dx.doi.org/10.1029/2006pa001355.
Jenkyns, H.C., Dickson, A.J., Ruhl, M., van den Boorn, S.H.J.M., 2017. Basalt–seawater interaction, the Plenus Cold Event, enhanced weathering and geochemical change: deconstructing Oceanic Anoxic Event 2 (Cenomanian–Turonian, Late Cretaceous). Sedimentology 64:16–43. http://dx.doi.org/10.1111/sed.12305.
Jilbert, T., Slomp, C.P., 2013. Rapid high-amplitude variability in Baltic Sea hypoxia during the Holocene. Geology 41:1183–1186. http://dx.doi.org/10.1130/G34804.1.
Jones, C.E., Jenkyns, H.C., 2001. Seawater strontium isotopes, oceanic anoxic events, and seafloor hydrothermal activity in the Jurassic and Cretaceous. Am. J. Sci. 301: 112–149. http://dx.doi.org/10.2475/ajs.301.2.112.
Jones, E.J.W., Bigg, G.R., Handoh, I.C., Spathopoulos, F., 2007. Distribution of deep-sea black shales of Cretaceous age in the eastern Equatorial Atlantic from seismic profiling. Palaeogeogr. Palaeoclimatol. Palaeoecol. 248:233–246. http://dx.doi.org/10.1016/j.palaeo.2006.12.006.
Junium, C.K., Freeman, K.H., Arthur, M.A., 2015. Controls on the stratigraphic distribution and nitrogen isotopic composition of zinc, vanadyl and free base porphyrins through Oceanic Anoxic Event 2 at Demerara Rise. Org. Geochem. 80:60–71. http://dx.doi.org/10.1016/j.orggeochem.2014.10.009.
Keller, G., Adatte, T., Berner, Z., Chellai, E.H., Stueben, D., 2008. Oceanic events and biotic effects of the Cenomanian-Turonian anoxic event, Tarfaya Basin, Morocco. Cretac. Res. 29:976–994. http://dx.doi.org/10.1016/j.cretres.2008.05.020.
Kennedy, H.A., Elderfield, H., 1987a. Iodine diagenesis in non-pelagic deep-sea sediments. Geochim. Cosmochim. Acta 51:2505–2514. http://dx.doi.org/10.1016/0016-7037(87)90301-2.
Kennedy, H.A., Elderfield, H., 1987b. Iodine diagenesis in pelagic deep-sea sediments. Geochim. Cosmochim. Acta 51:2489–2504. http://dx.doi.org/10.1016/0016-7037(87)90300-0.
Kerr, A.C., 1998. Oceanic plateau formation: a cause of mass extinction and black shale deposition around the Cenomanian-Turonian boundary? J. Geol. Soc. 155:619–626. http://dx.doi.org/10.1144/gsjgs.155.4.0619.
Knapp, G., Maichin, B., Fecher, P., Hasse, S., Schramel, P., 1998. Iodine determination in biological materials: options for sample preparation and final determination. J. Anal. Chem. 362:508–513. http://dx.doi.org/10.1007/s002160051116.
Kolonic, S., Wagner, T., Forster, A., Sinninghe Damsté, J.S., Walsworth-Bell, B., Erba, E., Turgeon, S., Brumsack, H.-J., Chellai, E.H., Tsikos, H., Kuhnt, W., Kuypers, M.M.M., 2005. Black shale deposition on the northwest African Shelf during the Cenomanian/Turonian oceanic anoxic event: climate coupling and global organic carbon burial. Paleoceanography 20, PA1006. http://dx.doi.org/10.1029/2003PA000950.
Kuhnt, W., Wiedmann, J., 1995. Cenomanian-Turonian source rocks: paleobiogeographic and paleoenvironmental aspects. In: Huc, A.Y. (Ed.), Palaeogeography, Paleoclimate, and Source Rocks. AAPG Studies in Geology 40, pp. 213–231.
Kuhnt, W., Luderer, F., Nederbragt, S., Thurow, J., Wagner, T., 2005. Orbital-scale record of the late Cenomanian-Turonian oceanic anoxic event (OAE-2) in the Tarfaya Basin (Morocco). Int. J. Earth Sci. 94:147–159. http://dx.doi.org/10.1007/s00531-004-0440-5.
Kuroda, J., Ogawa, N.O., Tanimizu, M., Coffin, M.F., Tokuyama, H., Kitazato, H., Ohkouchi, N., 2007. Contemporaneous massive subaerial volcanism and late cretaceous Oceanic Anoxic Event 2. Earth Planet. Sci. Lett. 256:211–223. http://dx.doi.org/10.1016/j.epsl.2007.01.027.
Kuypers, M.M.M., Pancost, R.D., Nijenhuis, I.A., Damste, J.S.S., 2002. Enhanced productivity led to increased organic carbon burial in the euxinic North Atlantic basin during the late Cenomanian oceanic anoxic event. Paleoceanography 17:1051. http://dx.doi.org/10.1029/2000pa000569.
Lancelot, Y., Seibold, E., Cepek, P., Dean, W.E., Eremeev, V., Gardner, J., Jansa, L.F., Johnson, D., Krasheninnikov, V., Pflaumann, U., Rankin, J.G., Trabant, P., Bukry, D., 1977. Site 367: Cape Verde Basin: Deep Sea Drilling Project Initial Reports. 41:pp. 163–232. http://dx.doi.org/10.2973/dsdp.proc.41.103.1978.
Lanci, L., Muttoni, G., Erba, E., 2010. Astronomical tuning of the Cenomanian Scaglia Bianca Formation at Furlo, Italy. Earth Planet. Sci. Lett. 292:231–237. http://dx.doi.org/10.1016/j.epsl.2010.01.041.
Leine, L., 1986. Geology of the Tarfaya oil shale deposit, Morocco. Geol. Mijnb. 65, 57–74.
Lu, Z., Hensen, C., Fehn, U., Wallmann, K., 2008. Halogen and 129I systematics in gas hydrate fields at the northern Cascadia margin (IODP Expedition 311): insights from numerical modeling. Geochem. Geophys. Geosyst. 9, Q10006. http://dx.doi.org/10.1029/2008GC002156.
Lu, Z., Jenkyns, H.C., Rickaby, R.E.M., 2010. Iodine to calcium ratios in marine carbonate as a paleo-redox proxy during oceanic anoxic events. Geology 38:1107–1110. http://dx.doi.org/10.1130/G31145.1.
Lu, Z., Hoogakker, B.A.A., Hillenbrand, C., Zhou, X., Thomas, E., Gutchess, K.M., Lu, W., Jones, L., Rickaby, R.E.M., 2016. Oxygen depletion recorded in upper waters of the glacial Southern Ocean. Nat. Commun.:7 http://dx.doi.org/10.1038/ncomms11146.
Ma, C., Meyers, S.R., Sageman, B.B., Singer, B.S., Jicha, B.R., 2014. Testing the astronomical time scale for oceanic anoxic event 2, and its extension into Cenomanian strata of the Western Interior Basin (USA). GSA Bull. 126:974–989. http://dx.doi.org/10.1130/B30922.1.
Mitchell, R.N., Bice, D.M., Montanari, A., Cleaveland, L.C., Christianson, K.T., Coccioni, R., Hinnov, L.A., 2008. Oceanic anoxic cycles? Orbital prelude to the Bonarelli Level (OAE 2). Earth Planet. Sci. Lett. 267:1–16. http://dx.doi.org/10.1016/j.epsl.2007.11.026.
Monteiro, F.M., Pancost, R.D., Ridgwell, A., Donnadieu, Y., 2012. Nutrients as the dominant control on the spread of anoxia and euxinia across the Cenomanian-Turonian oceanic anoxic event (OAE 2): model-data comparison. Paleoceanography 27, PA4209. http://dx.doi.org/10.1029/2012pa002351.
Mort, H., Jacquat, O., Adatte, T., Steinmann, P., Föllmi, K., Matera, V., Berner, Z., Stüben, D., 2007a. The Cenomanian/Turonian anoxic event at the Bonarelli Level in Italy and Spain: enhanced productivity and/or better preservation? Cretac. Res. 28:597–612. http://dx.doi.org/10.1016/j.cretres.2006.09.003.
Mort, H.P., Adatte, T., Follmi, K.B., Keller, G., Steinmann, P., Matera, V., Berner, Z., Stuben, D., 2007b. Phosphorus and the roles of productivity and nutrient recycling during oceanic anoxic event 2. Geology 35:483–486. http://dx.doi.org/10.1130/G23475a.1.
Muramatsu, Y., Wedepohl, K.H., 1998. The distribution of iodine in the earth's crust. Chem. Geol. 147:201–216. http://dx.doi.org/10.1016/S0009-2541(98)00013-8.
Murphy, D.P., Thomas, D.J., 2012. Cretaceous deep-water formation in the Indian sector of the Southern Ocean. Paleoceanography 27, PA1211. http://dx.doi.org/10.1029/2011PA002198.
Nederbragt, A.J., Thurow, J., Pearce, R., 2007. Sediment composition and cyclicity in the Mid-Cretaceous at Demerara Rise, ODP Leg 207. Proc. ODP Sci. Results 207:1–31. http://dx.doi.org/10.2973/odp.proc.sr.207.103.2007.
Noordmann, J., Weyer, S., Montoya-Pino, C., Dellwig, O., Neubert, N., Eckert, S., Paetzel, M., Bottcher, M.E., 2015. Uranium and molybdenum isotope systematics in modern euxinic basins: case studies from the central Baltic Sea and the Kyllaren fjord (Norway). Chem. Geol. 396:182–195. http://dx.doi.org/10.1016/j.chemgeo.2014.12.012.
Owens, J.D., Reinhard, Christopher T., Rohrssen, Megan, Love, Gordon D., Lyons, Timothy W., 2016. Empirical links between trace metal cycling and marine microbial ecology during a large perturbation to Earth's carbon cycle. Earth Planet. Sci. Lett. 449: 407–417. http://dx.doi.org/10.1016/j.epsl.2016.05.046.
Owens, J.D., Lyons, T.W., Hardisty, D.S., Lowery, C., Lu, Z., Lee, B., Jenkyns, H.C., 2017. Patterns of local and global redox variability during the Cenomanian–Turonian Boundary Event (Oceanic Anoxic Event 2) recorded in carbonates and shales from central Italy. Sedimentology 64:168–185. http://dx.doi.org/10.1111/sed.12352.
Pancost, R.D., Crawford, N., Magness, S., Turner, A., Jenkyns, H.C., Maxwell, J.R., 2004. Further evidence for the development of photic-zone euxinic conditions during Mesozoic oceanic anoxic events. J. Geol. Soc. 161:353–364. http://dx.doi.org/10.1144/0016764903-059.
Pogge von Strandmann, P.A.E., Jenkyns, H.C., Woodfine, R.G., 2013. Lithium isotope evidence for enhanced weathering during Oceanic Anoxic Event 2. Nat. Geosci. 6: 668–672. http://dx.doi.org/10.1038/ngeo1875.
Poulton, S.W., Canfeld, D.E., 2011. Ferruginous conditions: a dominant feature of the ocean through Earth's history. Elements 7:107–112. http://dx.doi.org/10.2113/gselements.7.2.107.
Poulton, S.W., Canfield, D.E., 2005. Development of a sequential extraction procedure for iron: implications for iron partitioning in continentally derived particulates. Chem. Geol. 214:209–221. http://dx.doi.org/10.1016/j.chemgeo.2004.09.003.
Poulton, S.W., Henkel, S., März, C., Urquhart, H., Flögel, S., Kasten, S., Sinninghe Damsté, J.S., Wagner, T., 2015. A continental-weathering control on orbitally driven redox-nutrient cycling during Cretaceous Oceanic Anoxic Event 2. Geology 43:963–966. http://dx.doi.org/10.1130/G36837.1.
Price, N.B., Calvert, S.E., 1973. Geochemistry of iodine in oxidized and reduced recent marine sediments. Geochim. Cosmochim. Acta 37:2149–2158. http://dx.doi.org/10.1016/0016-7037(73)90013-6.
Price, N.B., Calvert, S.E., 1977. The contrasting geochemical behaviours of iodine and bromine in recent sediments from the Namibian shelf. Geochim. Cosmochim. Acta 41 (12):1769–1775. http://dx.doi.org/10.1016/0016-7037(77)90209-5.
Price, N.B., Calvert, S.E., Jones, P.G.W., 1970. The distribution of iodine and bromine in the sediments of the Southwestern Barents Sea. J. Mar. Res. 28, 22–34.
Raiswell, R., Canfield, D.E., 1998. Sources of iron for pyrite formation in marine sediments. Am. J. Sci. 298:219–245. http://dx.doi.org/10.2475/ajs.298.3.219.
Reolid, M., Sánchez-Quiñónez, C.a., Alegret, L., Molina, E., 2015. Palaeoenvironmental turnover across the Cenomanian-Turonian transition in Oued Bahloul, Tunisia: foraminifera and geochemical proxies. Palaeogeogr. Palaeoclimatol. Palaeoecol. 417: 491–510. http://dx.doi.org/10.1016/j.palaeo.2014.10.011.
Rhoads, D.C., Morse, J.W., 1971. Evolutionary and ecologic significance of oxygen-deficient marine basins. Lethaia 4:413–428. http://dx.doi.org/10.1111/j.1502-3931.1971.tb01864.x.
Robbins, L.J., Lalonde, S.V., Planavsky, N.J., Partin, C.A., Reinhard, C.T., Kendall, B., Scott, C., Hardisty, D.S., Gill, B.C., Alessi, D.S., Dupont, C.L., 2016. Trace elements at the intersection of marine biological and geochemical evolution. Earth Sci. Rev. 163:323–348. http://dx.doi.org/10.1016/j.earscirev.2016.10.013.
Romarís-Hortas, V., Moreda-Piñeiro, A., Bermejo-Barrera, P., 2009. Microwave assisted extraction of iodine and bromine from edible seaweed for inductively coupled plasma-mass spectrometry determination. Talanta 79:947–952. http://dx.doi.org/10.1016/j.talanta.2009.05.036.

Rue, E.L., Smith, G.J., Cutter, G.A., Bruland, K.W., 1997. The response of trace element redox couples to suboxic conditions in the water column. Deep. Res. Part I-Oceanographic Res. Pap. 44, 113–134.

Schlanger, S.O., Jenkyns, H.C., 1976. Cretaceous oceanic anoxic events: causes and consequences. Geol. Mijnb. 55, 179–194.

Schlanger, S.O., Arthur, M.A., Jenkyns, H.C., Scholle, P.A., 1987. The Cenomanian–Turonian oceanic anoxic event, I. Stratigraphy and distribution of organic carbo-rich beds and the marine delta 13C excursion. In: Brooks, J., Fleet, A.J. (Eds.), Marine Petroleum Source Rocks. Blackwell Scientific Publications:pp. 371–399 http://dx.doi.org/10.1144/GSL.SP.1987.026.01.24.

Scopelliti, G., Bellanca, A., Neri, R., Baudin, F., Coccioni, R., 2006. Comparative high-resolution chemostratigraphy of the Bonarelli Level from the reference Bottaccione section (Umbria–Marche Apennines) and from an equivalent section in NW Sicily: Consistent and contrasting responses to the OAE2. Chem. Geol. 228:266–285. http://dx.doi.org/10.1016/j.chemgeo.2005.10.010.

Sinninghe Damsté, J.S., Köster, J., 1998. A euxinic southern North Atlantic Ocean during the Cenomanian/Turonian oceanic anoxic event. Earth Planet. Sci. Lett. 158: 165–173. http://dx.doi.org/10.1016/S0012-821X(98)00052-1.

Takashima, R., Nishi, H., Hayashi, K., Okada, H., Kawahata, H., Yamanaka, T., Fernando, A.G., Mampuku, M., 2009. Litho-, bio- and chemostratigraphy across the Cenomanian/Turonian boundary (OAE 2) in the Vocontian Basin of southeastern France. Palaeogeogr. Palaeoclimatol. Palaeoecol. 273:61–74. http://dx.doi.org/10.1016/j.palaeo.2008.12.001.

Tinggi, U., Schoendorfer, N., Davies, P.S.W., Scheelings, P., Olszowy, H., 2011. Determination of iodine in selected foods and diets by inductively coupled plasma-mass spectrometry. Pure Appl. Chem. 84:291–299. http://dx.doi.org/10.1351/PAC-CON-11-08-03.

Topper, R.P.M., Alexandre, J.T., Tuenter, E., Meijer, P.T., 2011. A regional ocean circulation model for the mid-Cretaceous North Atlantic Basin: implications for black shale formation. Clim. Past 7:277–297. http://dx.doi.org/10.5194/cp-7-277-2011.

Tribovillard, N., Algeo, T.J., Baudin, F., Riboulleau, A., 2012. Analysis of marine environmental conditions based onmolybdenum–uranium covariation—applications to Mesozoic paleoceanography. Chem. Geol. 324:46–58. http://dx.doi.org/10.1016/j.chemgeo.2011.09.009.

Tsikos, H., Jenkyns, H.C., Walsworth-Bell, B., Petrizzo, M.R., Forster, A., Kolonic, S., Erba, E., Silva, I.P., Baas, M., Wagner, T., and Damste, J.S.S., 2004, Carbon-isotope stratigraphy recorded by the Cenomanian-Turonian Oceanic Anoxic Event: correlation and implications based on three key localities: J. Geol. Soc., 161, p. 711–719, doi: 10.1144/0016-764903-077.

Tsunogai, S., 1971. Iodine in the deep water of the ocean. Deep Sea Research and Oceanographic Abstracts 18:913–919. http://dx.doi.org/10.1016/0011-7471(71)90065-9.

Tsunogai, S., Sase, T., 1969. Formation of iodide-iodine in the ocean. Deep-Sea Res. 16: 489–496. http://dx.doi.org/10.1016/0011-7471(69)90037-0.

Tullai, S., Tubbs, L.E., Fehn, U., 1987. Iodine extraction from petroleum for analysis of I-129/I-127 ratios by Ams. Nuclear Instruments & Methods in Physics Research Section B-Beam Interactions with Materials and Atoms 29:383–386. http://dx.doi.org/10.1016/0168-583X(87)90269-2.

Turgeon, S., Brumsack, H.-J., 2006. Anoxic vs dysoxic events reflected in sediment geochemistry during the Cenomanian–Turonian Boundary Event (Cretaceous) in the Umbria–Marche Basin of central Italy. Chem. Geol. 234:321–339. http://dx.doi.org/10.1016/j.chemgeo.2006.05.008.

Turgeon, S.C., Creaser, R.A., 2008. Cretaceous oceanic anoxic event 2 triggered by a massive magmatic episode. Nature 454:323–329. http://dx.doi.org/10.1038/Nature07076.

Ullman, W.J., Aller, R.C., 1985. The geochemistry of iodine in near-shore carbonate sediments. Geochim. Cosmochim. Acta 49:967–978. http://dx.doi.org/10.1016/0016-7037(85)90311-4.

Waite, T.J., Truesdale, V.W., 2003. Iodate reduction by *Isochrysis galbana* is relatively insensitive to de-activation of nitrate reductase activity - are phytoplankton really responsible for iodate reduction in seawater? Mar. Chem. 81:137–148. http://dx.doi.org/10.1016/s0304-4203(03)00013-6.

Westermann, S., Caron, M., Fiet, N., Fleitmann, D., Matera, V., Adatte, T., Föllmi, K.B., 2010. Evidence for oxic conditions during oceanic anoxic event 2 in the northern Tethyan pelagic realm. Cretac. Res. 31 (5):500–514. http://dx.doi.org/10.1016/j.cretres.2010.07.001.

Westermann, S., Vance, D., Cameron, V., Archer, C., Robinson, S.A., 2014. Heterogeneous oxygenation states in the Atlantic and Tethys oceans during Oceanic Anoxic Event 2. Earth Planet. Sci. Lett. 404:178–189. http://dx.doi.org/10.1016/j.epsl.2014.07.018.

Wong, G.T.F., 1980. The stability of dissolved inorganic species of iodine in seawater. Mar. Chem. 9:13–24. http://dx.doi.org/10.1016/0304-4203(80)90003-1.

Wong, G.T.F., Brewer, P.G., Spencer, D.W., 1976. The distribution of particulate iodine in the Atlantic Ocean. Earth Planet. Sci. Lett. 32:441–450. http://dx.doi.org/10.1016/0012-821X(76)90084-4.

Zhou, X., Jenkyns, H.C., Owens, J.D., Junium, C.K., Zheng, X., Sageman, B.B., Hardisty, D.S., Lyons, T.W., Ridgwell, A., Lu, Z., 2015. Upper ocean oxygenation dynamics from I/Ca ratios during the Cenomanian-Turonian OAE 2. Paleoceanography 30:510–526. http://dx.doi.org/10.1002/2014PA002741.